Kovove Mater. 50 2012 285–294
DOI: 10.4149/km_2012_4_285

Cracking of welded joints made of steel X10CrMoVNb9-1 (T91) – case study

M. Łomozik*, M. Zeman, R. Jachym

Testing of Materials Weldability and Welded Constructions Department, Instytut Spawalnictwa (Institute of Welding), ul. Bł. Czesława 16–18, 44-100 Gliwice, Poland

Received 18 August 2011, received in revised form 2 November 2011, accepted 15 November 2011

Abstract

The article describes the cracking of argon-welded TIG-welded circumferential butt joints of light-wall tubes made of steel X10CrMoVNb9-1 (T91), using filler metal C9 MV-IG. Fragments of welded joints and weld deposits underwent macro- and microscopic metallographic examination involving light microscopy. The investigation also involved tests of mechanical properties, impact energy and hardness, as well as chemical composition analyses. Structural tests of the areas containing cracks revealed the presence of high-temperature ferrite delta (ferrite δ). It was determined that the cracks in the welds of circumferential butt joints were caused by too high yield point and tensile strength of the weld metal not subjected to heat treatment (if compared with the corresponding properties of steel T91). The publication also provides technological recommendations specifying how to prevent the formation of cracks in such types of welded joints.

K e y w o r d s: martensitic steel, welding, welded joint, microstructure, cracking

1. Introduction

The development of thermal power engineering towards the applications utilising higher steam temperatures and thus obtaining higher efficiency is, first of all, conditioned by the availability of appropriate structural materials. The major elements of the boiler part of the power unit are retaining walls made of light-wall tubes, superheaters and steam resuperheaters, fresh steam heavy-wall tubes, etc. The requirements such elements must meet include formability, weldability and thermal workability. In addition, structural steels should also be characterised by mechanical properties enabling long-term operation at high temperature (creep strength) and allowing for the loading cyclicity (resistance to low-cycle thermal fatigue).

Since late 1980's one of the most popular creep-resisting steels used in the construction of power generation systems is steel X19CrMoVNb9-1 (T91).

The T91 steel owes its popularity mainly to its highest allowed operating stresses in the 600–625 ℃ temperature range. The article describes the cracking of circumferential butt welded joints of light-wall tubes made of steel X10CrMoVNb9-1 (T91).

2. Experimental material and objective of research

Circumferential butt joints made of the X10CrMoVNb9-1 (T91) steel were argon-shielded TIG-welded (141) on light-wall tubes (outer diameter ø 38 mm, wall thickness 5.6 mm), using Böhler-made filler metal C9 MV-IG (ø 2.4 mm) recommended for welding T91 steel [1]. All the joints were welded under identical conditions and differed only in cracks. The joints were welded in the vertical position (PF), with cracks occurring during the closure of a fusion layer – practically in the flat position. Welding was made in two layers, as shown in Fig. 1. After welding, the joints were not heat treated.

The specimens used in the tests were as follows:

a) fragments of circumferential butt welded joints of pipes designated 1, 2 and 4, and a fragment of a pipe

*Corresponding author: tel. +48 32 3358 328; fax +48 32 2314 652; e-mail address: Miroslaw.Lomozik@is.gliwice.pl

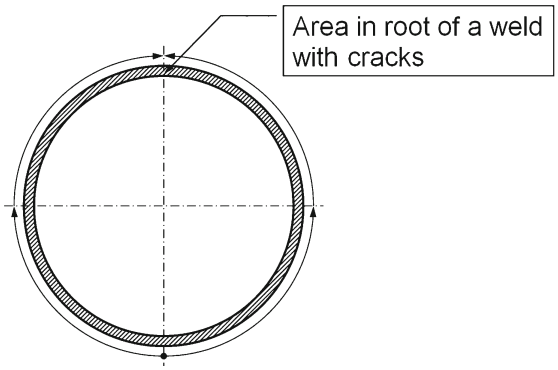

Fig. 1. Scheme of welding pipes made of T91 steel.

made of steel X10CrMoVNb9-1 (T91) designated BM (base metal) – Fig. 2a,

b) test plate of weld deposit not heat treated (designation WHT, i.e. without heat treatment) – Fig. 2b,

c) test plate of heat treated weld deposit (designation HT, i.e. heat treated) – Fig. 2c.

Cracks were present in the fragments of joints numbered 1 and 4. Joint no. 2 was free from cracks.

The objective of the tests was to determine the reason for crack formation in the welds of joints made of steel T91.

3. Procedure and test results

As the cracks found in some fragments of the test welded joints were located in the root of a weld and oriented across the weld (parallel to the longitudinal axis of the pipes being welded), metallographic microscopic specimens were prepared on the longitudinal section parallel to the main axis of the weld. The metallographic specimens were prepared pursuant to the requirements of the standard PN-EN 1321 [2], using a Buehler-manufactured grinding machine PowerPro 4000 as well as Struers and Buehler-made consumables.

The microstructure of the specimen material was revealed by means of $FeCl_3$ (etchant). The microscopic examination was carried out with a Leica-manufactured optical metallographic inverted microscope MeF4M. The tests of metallographic microscopic examinations are presented in Figs. 3 and 4 (joint no. 1), 5 and 6 (joint no. 2), as well as 7–9 (joint no. 4), respectively.

In low-carbon welds, ferrite δ is present in areas where temperature does not exceed 1350–1400 ℃. The amount of ferrite δ may increase [3, 4] with increasing speed of weld metal crystallisation followed by fast cooling. In the situation observed in the specimens, i.e. with martensite domination in the weld microstructure, presence of welding stresses as well as presence of

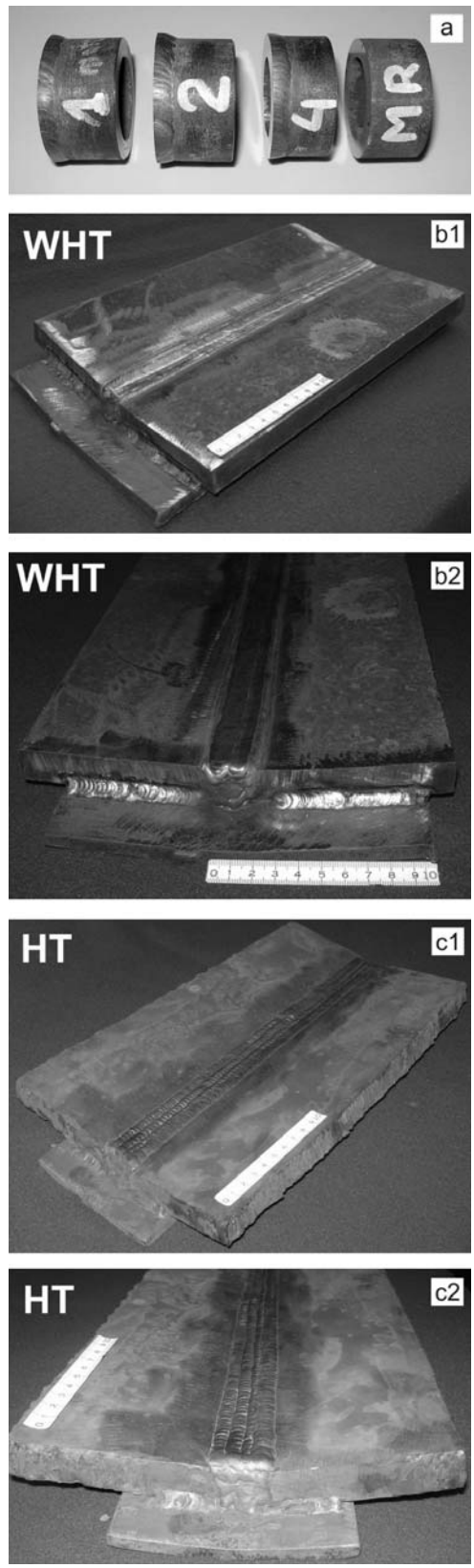

Fig. 2. Main view of specimens: a) fragments of circumferential butt welded joints and base metal of pipes made of T91 steel, b) test plate of weld deposit not heat treated, c) test plate of heat treated weld deposit.

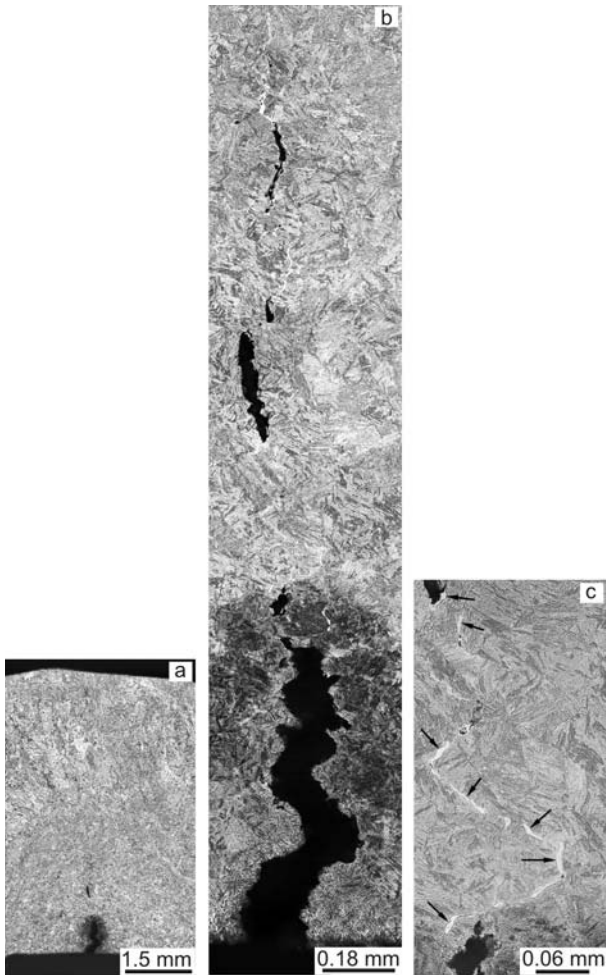

Fig. 3. Welded joint no. 1: a) main view of longitudinal section of circumferential butt weld with visible crack in root area; etch. $FeCl_3$, mag. 25×, b) course of crack; etch. $FeCl_3$, mag. 200×, c) area in which crack is present. Ferrite delta (δ) on boundaries of former austenite grains. Matrix – martensite; etch. $FeCl_3$, mag. 500×.

ferrite δ on the boundaries of former austenite grains, the areas favouring crack generation are those revealing ferrite presence; this being due to the fact that the mechanical properties of areas with ferrite δ are lower than those of surrounding martensite matrix. Moreover, in steels with higher chromium content (Cr content in steel T91 amounts to 8–9 %), ferrite is characterised by considerable brittleness, which in the case under discussion, additionally favours the generation of cracks in the areas containing ferrite. From a practical point of view, in order to prevent ferrite presence in weld metal after its solidification, it is recommended that post-weld joint cooling speed should be reduced (i.e. cooling time should be extended). Lower cooling speed will enable an increase in martensite volume fraction in the weld as more ferrite δ will transform into austenite and, following that, into martensite [4].

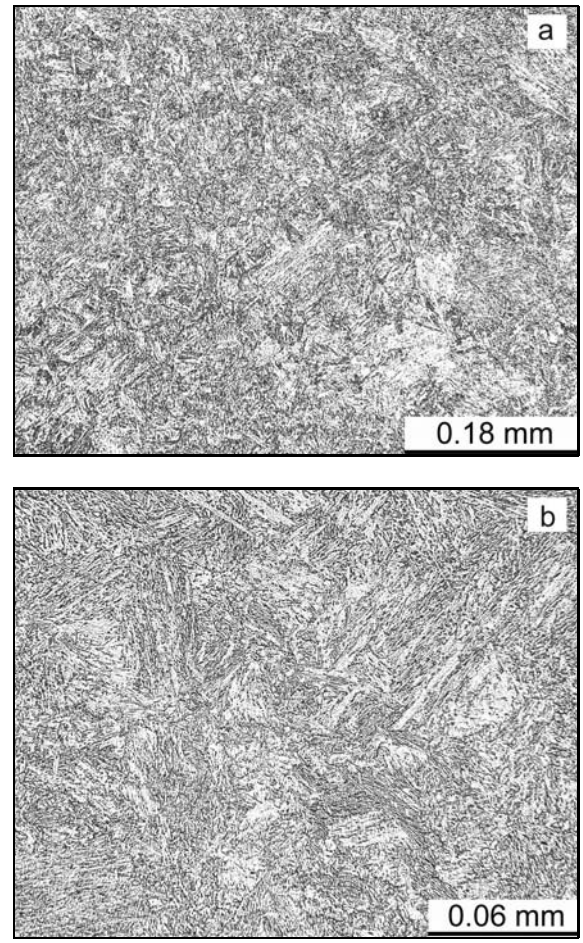

Fig. 4. Welded joint no. 1. Pipe area opposite to cracking area. Mixture of martensite and bainite: a) mag. 200×, b) mag. 500×, etch. $FeCl_3$.

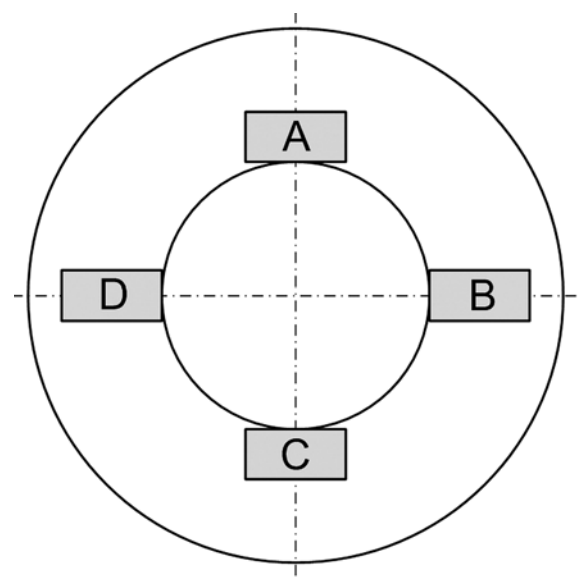

Fig. 5. Schematic presentation of areas for microscopic examination in welded joint no. 2 (without cracks).

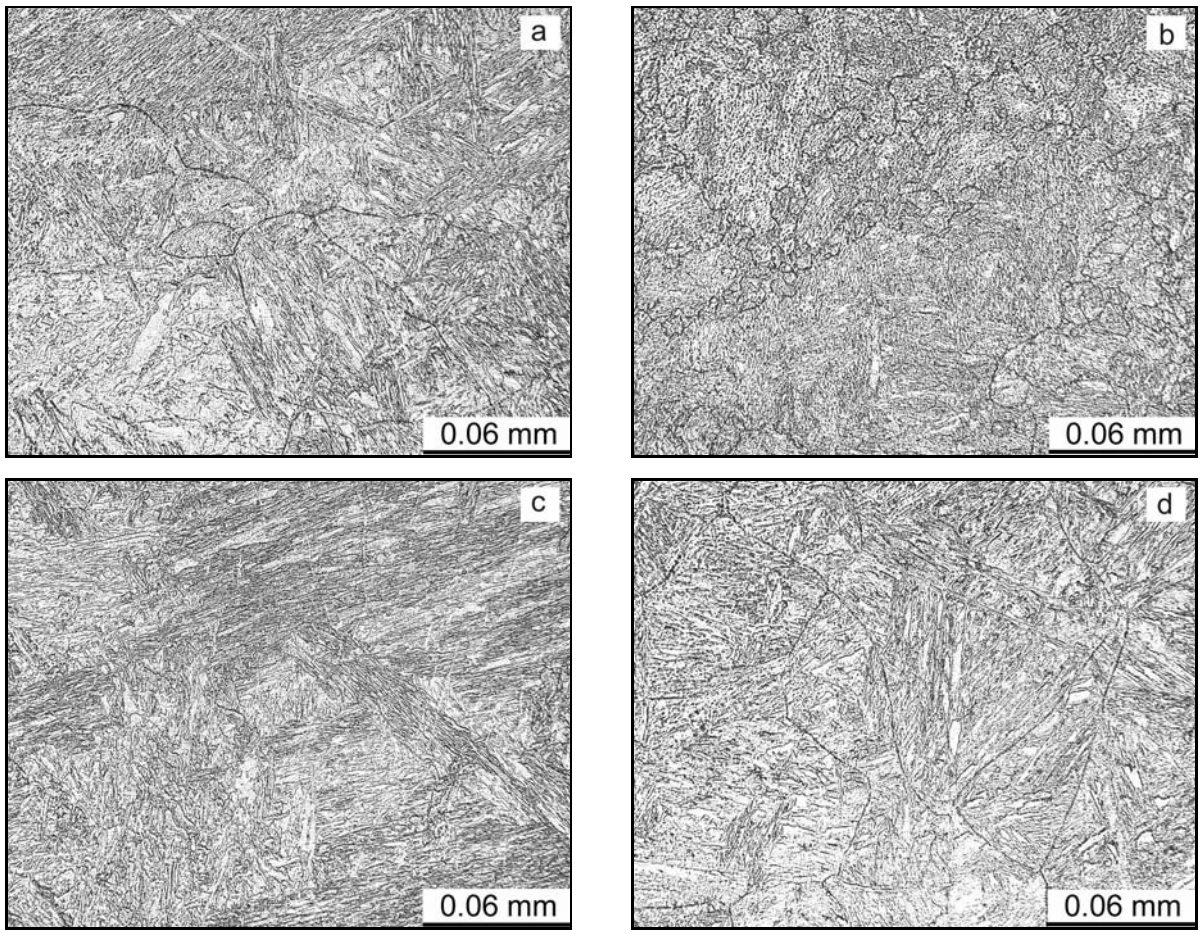

Fig. 6. Welded joint no. 2 without cracks. Test areas acc. to Fig. 5: a) A, b) B, c) C, d) D. Mixture of martensite and bainite; mag. 500×, etch. $FeCl_3$.

In welded joint no. 2 (free from cracks), metallographic microscopic tests focused on the areas of the root of the circumferential weld as presented in Fig. 5. The objective of the tests was to determine the morphology of the weld microstructure on the pipe circumference and to find differences, if any (Figs. 6–9).

The metallographic specimens made of joints no. 1, 2 and 4 were used to carry out Vickers hardness tests pursuant to the requirements of the standard PN-EN ISO 9015-1 [5] (see the scheme presented in Fig. 10); force of indenter load = 98.1 N (HV10).

List of hardness measurement results is presented in Fig. 11.

In order to more precisely determine the hardness values in areas located in the direct vicinity of the cracks, in samples nos. 1 and 4 micro-hardness measurements HV1 were conducted pursuant to the requirements of the standard PN-EN ISO 9015-2 [6]. The micro-hardness measurement results are presented in Fig. 12.

In the as delivery state the T91 steel [7], after quenching and tempering, should have a homogeneous microstructure of tempered martensite with elongated ferrite subgrains with a high dislocation density and numerous $M_{23}C_6$ type carbides precipitated on subgrain boundaries and high dispersive MX type carbonitrides.

The cross-section of a fragment of a pipe made of the steel X10CrMoVNb9-1, designated as BM (base metal), was used to prepare a metallographic specimen for microscopic examination, pursuant to the requirements of standard PN-EN 1321 [2]. The microstructure of the steel was revealed by means of $FeCl_3$ (etchant). The results of microscopic metallographic examination of the base metal of steel T91 are presented in Fig. 13.

The chemical composition of the weld deposit not subject to heat treatment and the one after heat treatment was determined with a Spectro-manufactured Spectrolab-type spark spectrometer (Germany), atomic absorption spectrometer (AAS) Perkin Elmer 330 (USA) and Japan's HORIBA-made Emia-type analyser for determining the contents of coal and sulphur. The process was conducted pursuant to relevant methods and determination of chemical element content. Nitrogen content was determined with a LECO analyser. The results of analyses are presented in Table 1.

The test plates (without heat treatment and heat

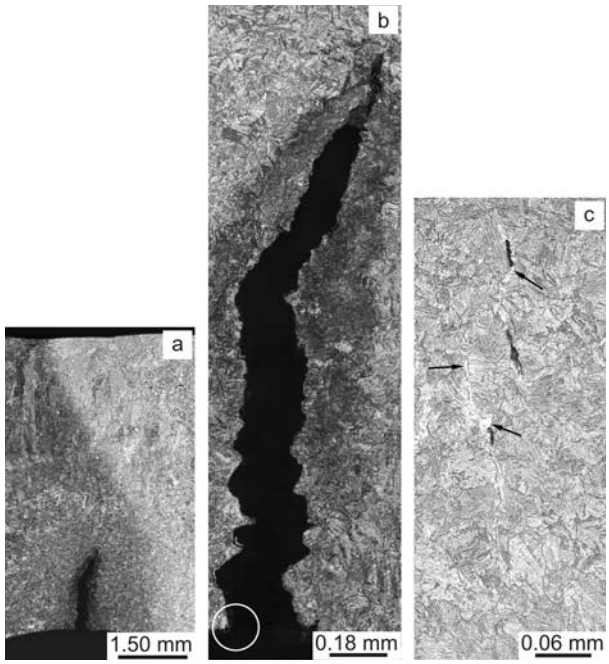

Fig. 7. Welded joint no. 4: a) main view of longitudinal section of circumferential butt weld with visible crack in the area of root of weld; etch. $FeCl_3$, mag. 25×, b) course of crack; etch. $FeCl_3$, mag. 200×, c) micro-cracks in weld near main crack. Ferrite δ visible on crack propagation line; etch. $FeCl_3$, mag. 500×.

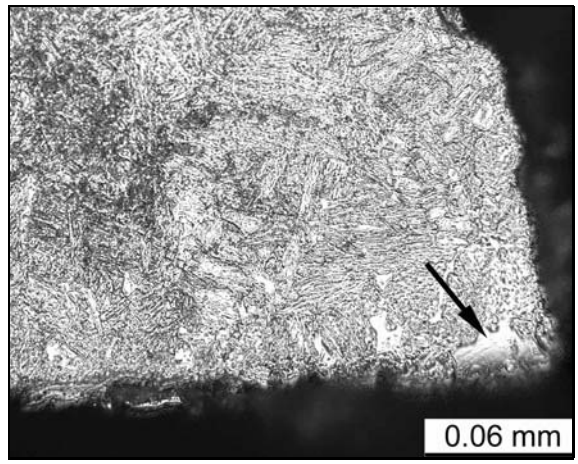

Fig. 8. Welded joint no. 4. Area near root of weld marked on Fig. 7b with visible ferrite δ; etch. $FeCl_3$, mag. 500×.

treated) were sampled for specimens to be used in the following mechanical tests: static tensile tests on circular section, impact tests at ambient temperature and lower temperatures, macroscopic metallographic tests and Vickers hardness tests. The weld deposit testing methods were selected pursuant to the standard PN-EN ISO 15792-1 [9].

The mechanical tests were conducted pursuant to the following standards:

– static tensile tests on longitudinal samples with circular section: acc. to the standard PN-EN 876 [10],

– impact tests: acc. to the standard PN-EN ISO 148-1 [11],

– macroscopic metallographic tests: acc. to the standard PN-EN 1321 [2],

– hardness measurements: acc. to the standard PN-EN ISO 9015-1 [5].

The results of static tensile tests on weld deposit not subjected to heat treatment and subjected to heat treatment are presented in Fig. 14. The results of impact tests on weld deposit at ambient temperature and lower temperatures are presented in Fig. 15. The results of macroscopic metallographic tests on weld deposit are presented in Fig. 16. The results of Vickers hardness tests (HV10) are presented in Fig. 17.

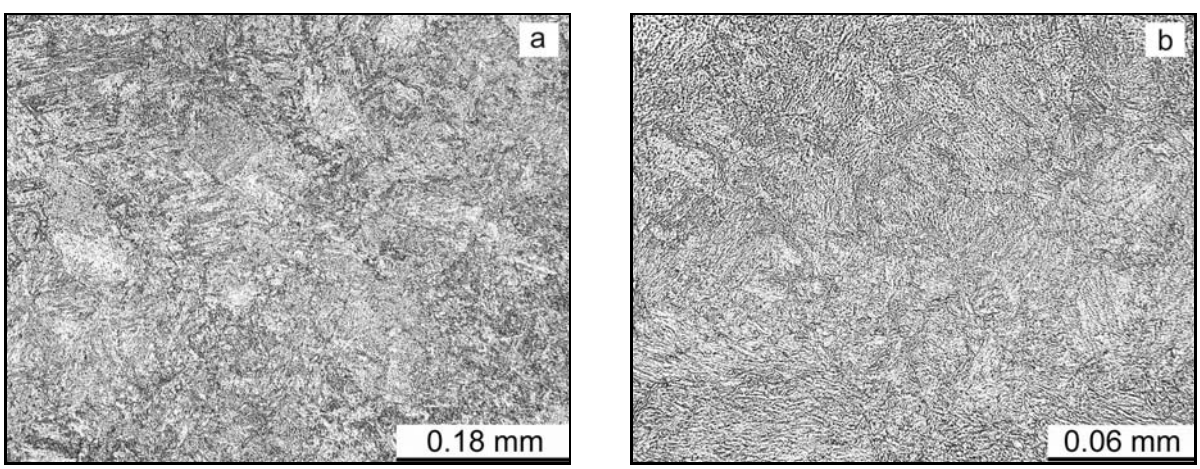

Fig. 9. Welded joint no. 4. Pipe area opposite to cracking area. Mixture of martensite and bainite: a) mag. 200×, b) mag. 500×, etch. $FeCl_3$.

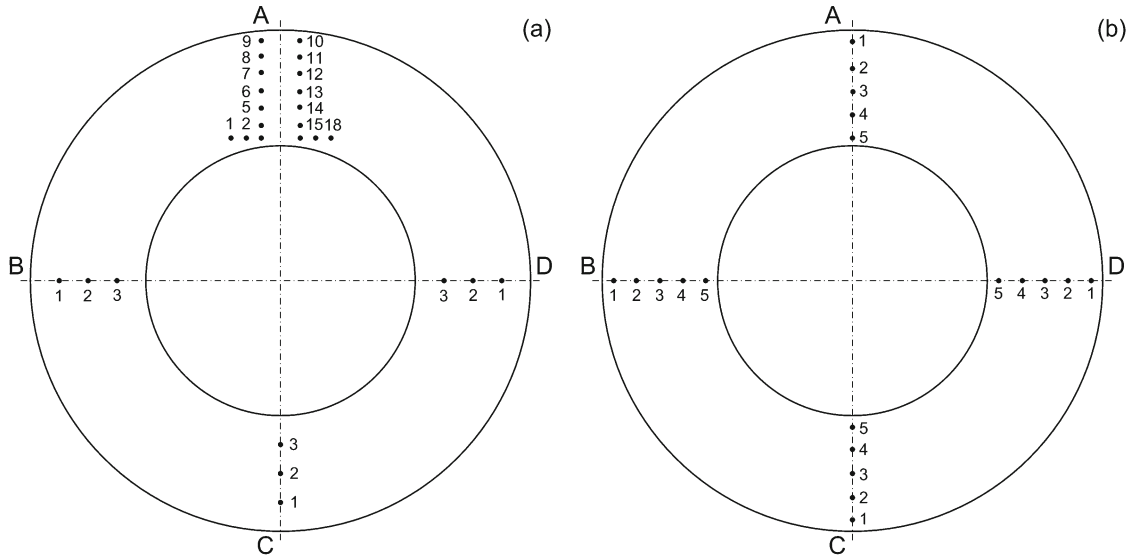

Fig. 10. Scheme of hardness measurement in samples: a) for samples nos. 1 and 4 (samples with cracks), b) for sample no. 2 and BM (samples without cracks).

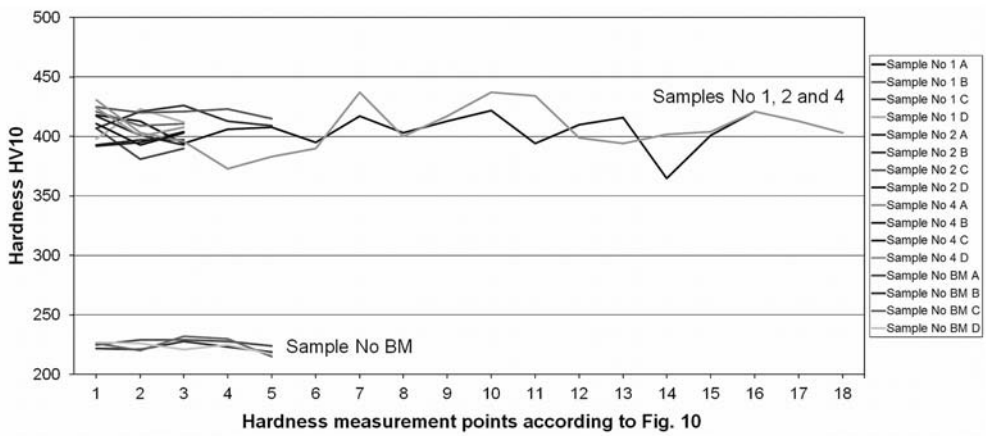

Fig. 11. Distribution of hardness in samples nos. 1, 2, 4 and BM.

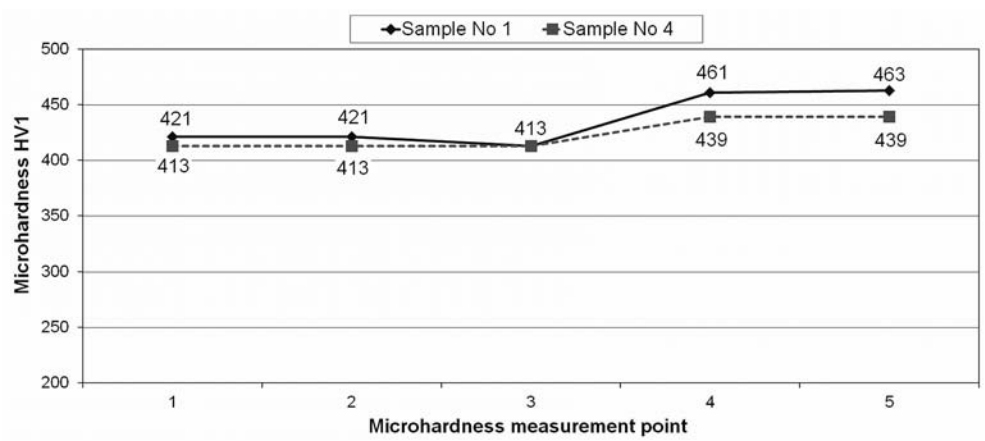

Fig. 12. Micro-hardness near cracks in samples nos. 1 and 4.

Table 1. Chemical composition of weld deposits under test, without heat treatment and subjected to heat treatment and acc. to welding filler metal manufacturer (Böhler)

		Chemical element content (%)															
	Element	C	Si	Mn	P	S	Cr	Mo	Ni	Nb	N	V	Cu	Al_{total}	W	Ti	B
Weld deposit	Without heat treatment	0.11	0.25	0.76	0.008	0.004	8.59	0.88	0.41	0.045	0.030	0.19	0.05	0.010	0.003	0.003	0.0001
	After heat treatment	0.11	0.25	0.76	0.008	0.004	8.92	0.87	0.41	0.047	0.023	0.20	0.05	0.008	0.001	0.003	0.0001
Acc. to [8]		0.115	0.26	0.76	0.006	0.002	8.95	0.99	0.47	0.060	0.033	0.197	0.04	–	–	–	–

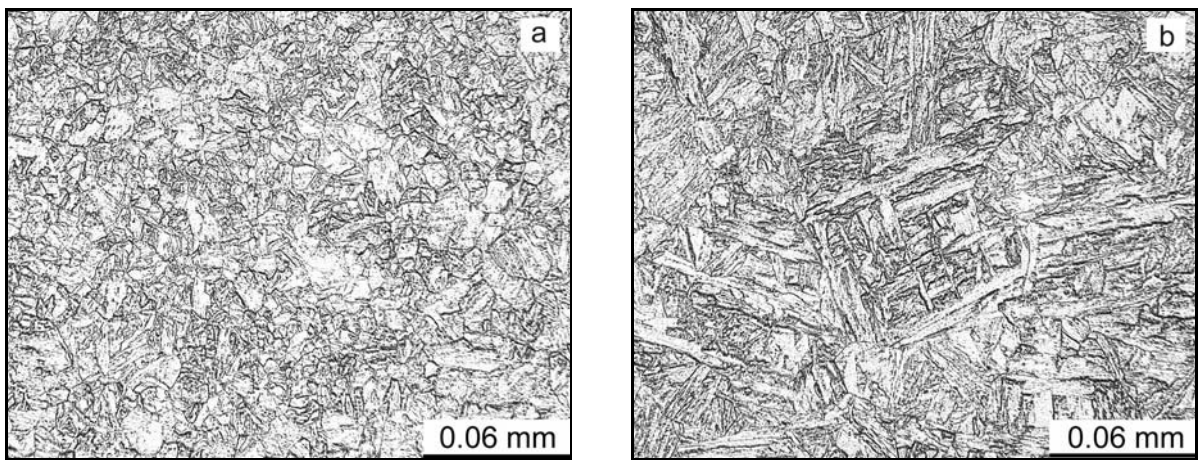

Fig. 13. Steel T91. Base metal: a) tempered martensite, b) area other than a). Martensite with expanded laths; mag. 500×, etch. $FeCl_3$.

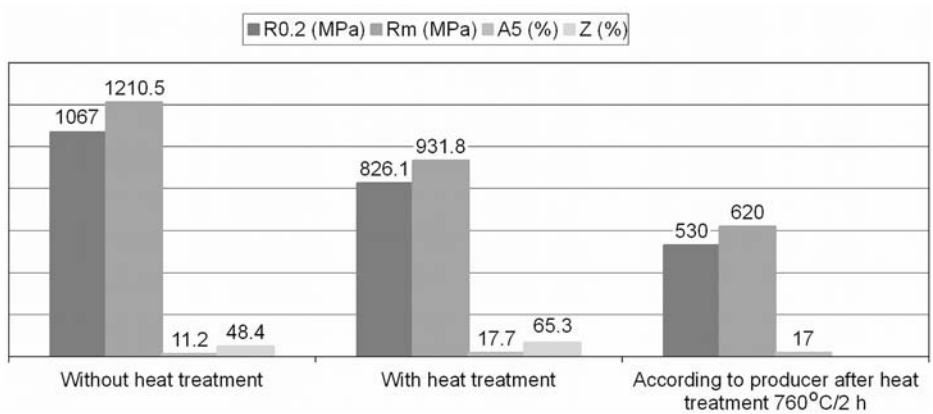

Fig. 14. Mechanical properties of weld deposit with and without heat treatment.

4. Discussion

Microscopic metallographic examinations conducted on fragments of the circumferential butt welded joints revealed that:

a) cracks in the area of the root of the weld were present in fragments nos. 1 and 4, whereas joint no. 2 was free from cracks,

b) cracks developed in the microstructure of martensite, along the trajectory indicated by the presence of ferrite δ located on the boundaries of packets of martensite laths (Figs. 3c, 7c and 8) and voids resulting from welding process imperfection (Fig. 3b),

c) weld metal microstructure was composed of martensite and the mixture of martensite and bainite.

In the fragment of the pipe made of steel T91 designated BM, it was possible to observe that the mi-

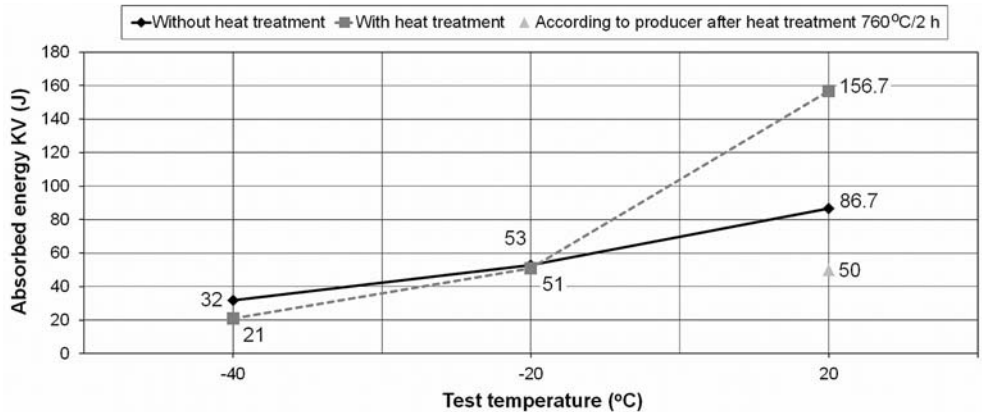

Fig. 15. Impact energy of weld deposit with and without heat treatment.

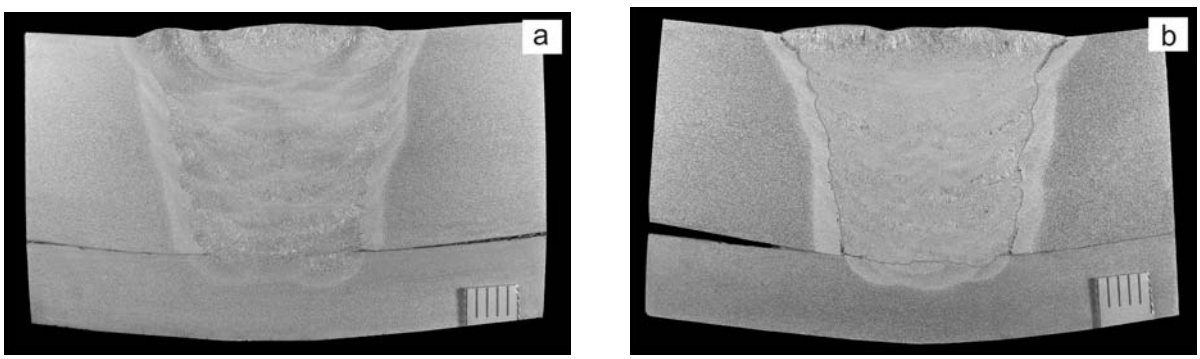

Fig. 16. Macrostructures of weld deposits: a) without heat treatment, b) with heat treatment; etch. Adler.

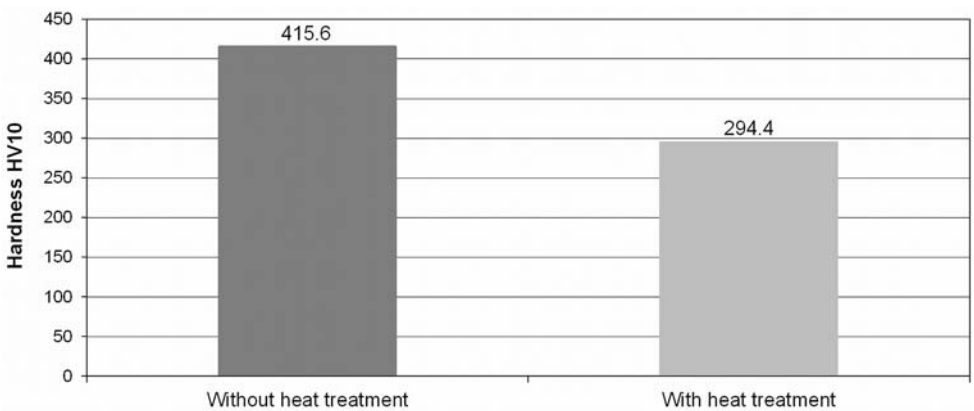

Fig. 17. Results of hardness measurements of weld deposit with and without heat treatment.

crostructure on the pipe circumference was heterogeneous. The predominant structure is that of tempered martensite (Fig. 13a), but locally one can also find areas of martensite with expanded laths (Fig. 13b). The differentiation of the morphology of the structure was not reflected in the hardness of the base metal, which changed only slightly in the 217–230 HV10 range and was contained in the allowed range specified by the steel producer (min. 200, max. 265 HV) [12]. In the fragment of welded joint no. 1, in the crack area in the weld, hardness values were between 413 and 463 HV1. In the remaining areas of sample no. 1, i.e. in the areas outside the crack, hardness values were between 381 and 423 HV10. In fragment no. 2 (i.e. the one without cracks), hardness values were between 392 and 426 HV10. In turn, in fragment no. 4, in the crack area, hardness value was between 413 and 439 HV1. In other areas of the weld in joint no. 4, hardness values were between 393 and 424 HV10. The diagram presented in Fig. 11 shows that hard-

ness values in fragments of welded joints no. 1, 2 and 4 are around 400 HV10, without significantly higher or lower peaks of values. In other words, hardness of the microstructures of welds under tests is stabilised.

The analysis of the chemical composition of the weld deposit subjected and not subjected to heat treatment showed no considerable deviations from the data contained in the certificate of the producer of filler metal in the form of TIG-welding rods C9 MV-IG [8].

The static tensile test involving the weld deposit revealed that the average values of yield point $R_{0.2}$ and tensile strength R_m of the weld deposit not subjected to heat treatment were 1067 and 1210 MPa, respectively. Heat treatment consisting in soaking the weld deposit at 760 ℃ for 2 h decreased the average yield point down to 826 MPa and tensile strength to about 932 MPa. Both with and without heat treatment, the mechanical properties of the weld deposits under test are higher than the minimum values of $R_{0.2}$ and R_m declared in the producer's certificate for the weld deposit of TIG-welding rods of C9 MV-IG grade; the said values being 530 and 620 MPa (Fig. 14), respectively. For comparison-related purposes one may assume that the mechanical properties of the weld in the welded joint without heat treatment, taking into consideration the degree of mixing of materials during welding, will be similar to the mechanical properties of the weld deposit without heat treatment. On the basis of the foregoing assumption it is possible to state that the mechanical properties of the weld in the welded joints under test were considerably higher than the mechanical properties of the base metal of steel T91 after quenching and tempering declared by the producer of the steel [12]. The average value of the yield point of the weld deposit not subjected to heat treatment amounted to 1067 MPa and was approximately 2.4 times higher than the minimum value of the yield point of steel T91 after quenching and tempering (450 MPa). In turn, the average value of the tensile strength of the weld deposit not subjected to heat treatment amounted to 1210 MPa and was approximately 1.4 times higher than the maximum value of the tensile strength of steel T91 recommended by the producer of the steel (850 MPa). Also the mechanical properties of the weld deposit subjected to heat treatment were significantly higher than those recommended by the producer both for the weld deposit and steel T91 (the average values of the mechanical properties of the weld deposit subjected to heat treatment: $R_{0.2} = 826$ MPa, $R_m = 931$ MPa). In turn, the average value of elongation A_5 of the weld deposit not subjected to heat treatment was considerably lower (11 %) than the value of elongation recommended by the producers both for the weld deposit obtained through TIG welding (A_5 = min. 17 %) and steel T91 (A_5 = min. 19 %).

The average values of impact energy of the weld deposit not subjected to heat treatment, tested at –40, –20 and +20 ℃, were 32, 53 and 87 J, respectively. The average values of impact energy of the weld deposit after heat treatment, tested at –40, –20 and +20 ℃, were 21, 51 and 157 J, respectively (Fig. 15).

High mechanical properties of the weld metal were the main reason for cracks located in the fragments of welded joints under test.

The publication [13] emphasizes that cracking in joints may be attributed to too high strength of the weld metal in relation to the strength of the base metal of steel T91. The reason for cracks is longitudinal welding stress. During the solidification and crystallisation of the weld metal, the latter undergoes longitudinal shrinkage and the base metal surrounding the weld area resists deformations, which results in the generation of compressive stresses in the base metal and tensile stresses in the weld [14]. Due to the too high yield point of the weld metal, the aforesaid stresses cannot undergo relaxation as a result of plastic deformations and, with insufficient plasticity of the weld metal, intercrystalline cracks are formed. The aforementioned cracks are located across the longitudinal axis of the weld (across the axis of the circumferential weld), along which high tensile shrinkage stresses are present.

The cracking in the fragments of welded joints under test is favoured by the presence of the martensitic microstructure of high hardness (approx. 460 HV1 in joint no. 1 and approx. 430 HV1 in joint no. 4) as well as by the presence of ferrite δ precipitates increasing the brittleness of the microstructure on grain boundaries and decreasing mechanical properties if compared with the strength of the matrix composed of martensite (Figs. 3c, 7c and 8).

The presence of welding imperfections while making the root of the weld favours crack generation. Very precise closure of the root of the weld (with the penetration of the previously made initial section of the back weld, application of accurate and impenetrable gas shield (Ar)) and limitation of the speed of post-weld cooling of the joint (by applying pre-heating and post-weld slow cooling) may significantly improve the quality of a weld.

Technological recommendations aimed at preventing crack formation:

a) selection of weld deposit for welding of steel T91 (wire C9 MV-IG) with the lower carbon content (within the allowed carbon content range) in order to improve the plastic properties of the weld metal;

b) pre-heating before welding up to 150–200 ℃ and post-weld heat treatment at 750 ℃, pursuant to the recommendations of Vallourec & Mannesmann Tubes [15];

c) reducing the speed of post-weld cooling of the

joint by applying heating mats, mineral wool mats etc.;

d) application of welding techniques with the closure of a circumferential weld with the so-called "lap".

5. Conclusions

On grounds of the tests it was possible to formulate the following conclusions:

1. In the microstructure, the crack-containing areas are dominated by martensite with a small amount of ferrite δ.

2. The maximum hardness values in the areas with cracks in the welded joints are 463 HV1 in sample no. 1 and 439 HV1 in sample no. 4.

3. In the welded joints, outside the areas with cracks, it is possible to observe the mixture of martensite and bainite of hardness values amounting to approx. 400 HV10.

4. The chemical composition of the weld deposit with and without heat treatment is consistent with the data provided in the certificate issued by the producer of rods for TIG welding of steel T91.

5. The values of the yield point and tensile strength of the weld deposit both without and after heat treatment are high and significantly exceed the values of corresponding properties recommended by the producers for the weld deposit and steel X10CrMoVNb9-1 (T91).

6. The basic reason for crack formation in the welds of TIG-welded circumferential butt joints (made using the C9 MV-IG rods) is too high value of the yield point and tensile strength of the weld metal not subjected to heat treatment if compared to the corresponding properties of the base metal of steel T91. High value of the yield point of the weld metal prevents the relaxation of tensile stresses resulting from the shrinkage of the weld during its solidification and crystallisation at the cooling stage, which, in turn, leads to the formation of transverse cracks.

7. Due to the high values of hardness in the weld, the application of pre-heating before welding and post-weld heat treatment of the joints may decrease the intensity of crack formation in the roots of TG-welded circumferential butt welds.

Acknowledgements

This work was supported by the Instytut Spawalnictwa research project No. Ia-26, 2010.

References

[1] Welding Guide. Böhler Welding. Kapfenberg, Böhler Schweißtechnik Austria GmbH, 2010, p. 135.
[2] PN-EN 1321:2000 Destructive tests on welds in metallic materials. Macroscopic and microscopic examination of welds.
[3] Węgrzyn, T.: Ferrite delta in steel acid-resistant welds. Bulletin of Instytut Spawalnictwa in Gliwice, 1992, *1*, p. 43.
[4] Tasak, E., Ziewiec, A.: Weldability of Steels. Volume 1. Kraków, Publishing House: JAK 2009.
[5] PN-EN ISO 9015-1:2011 Destructive tests on welds in metallic materials. Hardness testing. Part 1: Hardness test on arc welded joints.
[6] PN-EN ISO 9015-2:2011 Destructive tests on welds in metallic materials. Hardness testing. Part 2: Micro hardness testing on welded joints.
[7] ASTM A335 Seamless Ferritic Alloy Steel Pipe for High Temperature Service.
[8] Copy of certificate no. 2-2008-03-1493444 for rods used in TIG welding; grade: C9 MV-IG; producer: Böhler.
[9] PN-EN ISO 15792-1:2008/A1:2012 Welding consumables. Test methods. Part 1: Test methods for all-weld metal test specimens in steel, nickel and nickel alloys.
[10] PN-EN 876:1999 Destructive tests on welds in metallic materials. Longitudinal tensile test on weld metal in fusion welded joints.
[11] PN-EN ISO 148-1:2010 Metallic materials. Charpy pendulum impact test. Part 1: Test method.
[12] Copy of certificate no. 1097Sv10 for pipes made of steel T91 of Vallourec-Mannesmann Tubes.
[13] Weld cracking. An excerpt from the fabricator's and erector's guide to weld steel construction http://content.lincolnelectric.com/pdfs/knowledge/articles/content/weldcracking.pdf
[14] Tasak, E., Ziewiec, A.: Welding Review, *1*, 2007, p. 14.
[15] Haarmann, K., Vaillant, J. C., Vandenberghe, B., Bendick, W., Arbab, A.: The T91/P91 Book. Boulogne, Vallourec & Mannesmann Tubes 2002.